On making nD images well-composed by a self-dual local interpolation

Nicolas Boutry[1,2], Thierry Géraud[1], and Laurent Najman[2]

[1] EPITA Research and Development Laboratory (LRDE)
[2] Université Paris-Est, LIGM, Équipe A3SI, ESIEE
firstname.lastname@lrde.epita.fr, l.najman@esiee.fr

Abstract. Natural and synthetic discrete images are generally not well-composed, leading to many topological issues: connectivities in binary images are not equivalent, the Jordan Separation theorem is not true anymore, and so on. Conversely, making images well-composed solves those problems and then gives access to many powerful tools already known in mathematical morphology as the Tree of Shapes which is of our principal interest. In this paper, we present two main results: a characterization of 3D well-composed gray-valued images; and a counter-example showing that no local self-dual interpolation satisfying a classical set of properties makes well-composed images with one subdivision in 3D, as soon as we choose the mean operator to interpolate in 1D. Then, we briefly discuss various constraints that could be interesting to change to make the problem solvable in nD.

Keywords: Digital topology, gray-level images, well-composed sets, well-composed images

1 Introduction

Natural and synthetic images are usually not well-composed. This fact raises many topological issues. As an example, the Jordan Separation theorem, stating that a simple closed curve in $\mathbb{R}^2$ separates the space in only two components is not true anymore for binary 2D discrete images [5]. To solve this problem, we have to juggle with two complementary connectivities: 4 for the background and 8 for the foreground, or the inverse. 2D well-composed binary images have the fundamental property that 4- and 8-connectivities are equivalent. Hence, such topological issues vanish. In the same manner, well-composed nD images, with $n > 2$, have $2n$- and $(3^n - 1)$-connectivities equivalent [11]. Other advantages of well-composed images are for example the preservation of topological properties by a rigid transform [10], simplification of thinning algorithms [8] and simplification of graph structures resulting from skeleton algorithms [5]. Also, and it is our most important goal, one can compute the Tree of Shapes [9,2] of a well-composed image with a quasi-linear algorithm [3]. An introduction to the Tree of Shapes in the continuous case can be found in [1].

Section 2 recalls the definitions of 2D and 3D well-composed sets and gray-valued images, and introduces a characterization of 3D gray-valued well-composed images. Because we do not want to deteriorate the initial signal, we use an interpolation that produces a well-composed image. Furthermore, in order to treat in the same manner bright components on dark background and dark components over bright background, this interpolation process will be self-dual. We present in Section 3 a general scheme that recursively defines local interpolations satisfying a classical set of properties with one subdivision. We show that such interpolations, with the added property of being self-dual, fail in 3D (and then further) to make well-composed images. We conclude in Section 4 with some perspectives that could work in nD even if $n > 2$ (in local and non-local ways).

2 A characterization of 3D well-composed gray-valued images

2.1 2D WC Sets and Gray-Valued Images

Let us begin by the definitions of a block of $\mathbb{Z}^n$. We will then be able to recall the definition and the characterization of 2D well-composed sets and images.

A block in nD associated to $z \in \mathbb{Z}^n$ is the set S_z defined such that $S_z = \left\{z' \in \mathbb{Z}^n \middle| ||z - z'||_\infty \leq 1 \text{ and } \forall i \in [1,n], z'_i \geq z_i\right\}$ (where z_i represents the i^{th} coordinate of z). Moreover, we call blocks of $\mathcal{D} \subseteq \mathbb{Z}^n$ any element of the set $\left\{S_z \middle| \exists z \in \mathcal{D}, S_z \subseteq \mathcal{D}\right\}$.

Definition 1 (2D WC Sets [5]) *A set X is weakly well-composed if any 8-component of X is a 4-component. X is well-composed if both X and its complement $X^c = \mathbb{Z}^2 \setminus X$ are weakly well-composed.*

Proposition 1 (Local Connectivity and No Critical Configurations [5]) *A set $X \subseteq \mathbb{Z}^2$ is well-composed iff it is locally 4-connected. Also, a set X is well-composed if none of the critical configurations $\begin{pmatrix} 1 & 0 \\ 0 & 1 \end{pmatrix}$ or $\begin{pmatrix} 0 & 1 \\ 1 & 0 \end{pmatrix}$ appears in X.*

Definition 2 (Cuts in nD) *For any $\lambda \in \mathbb{R}$ and any gray-valued map $u : \mathcal{D} \subseteq \mathbb{Z}^n \mapsto \mathbb{R}$, we denote by $[u > \lambda]$ and $[u < \lambda]$ the sets $[u > \lambda] = \left\{M \in \mathcal{D} \middle| u(M) > \lambda\right\}$ and $[u < \lambda] = \left\{M \in \mathcal{D} \middle| u(M) < \lambda\right\}$. We call them respectively upper strict cuts and lower strict cuts [3].*

We remark that an image $u : \mathcal{D} \subseteq \mathbb{Z}^2 \mapsto \mathbb{R}$ with a finite domain $\mathcal{D}$ can only be well-composed if $\mathcal{D}$ is itself well-composed (since $[u < \max(u) + 1] = \mathcal{D}$).

Definition 3 (Gray-valued WC 2D Maps [5]) *A gray-level map $u : \mathbb{Z}^2 \mapsto \mathbb{R}$ is* well-composed *iff for every $\lambda \in \mathbb{R}$, the strict cuts $[u > \lambda]$ and $[u < \lambda]$ result in well-composed sets.*

We recall that the *interval value* of the couple $(x, y) \in \mathbb{R}^2$ is defined as $\text{intvl}(x, y) = [\min(x, y), \max(x, y)]$.

Proposition 2 (Characterization of 2D WC maps [5]) *A gray-level map* $u : \mathbb{Z}^2 \mapsto \mathbb{R}$ *is well-composed iff for every 2D block* S *such that* $u\big|_S = \begin{pmatrix} a & b \\ c & d \end{pmatrix}$, *the interval values satisfy* $\mathrm{intvl}(a,d) \cap \mathrm{intvl}(b,c) \neq \emptyset$.

2.2 3D WC Sets and Gray-Valued Maps

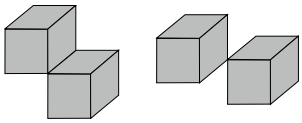

Fig. 1. Illustration of the bdCA of a set containing a critical configurations of type 1 (left), and of type 2 (right).

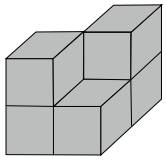

Fig. 2. A set locally 6-connected but not well-composed.

As we will see, for $n = 3$, the equivalence between local connectivity and well-composedness is no longer true. This led Latecki [4] to introduce the continuous analog.

Definition 4 (CA **and** bdCA **[4])** *The* continuous analog $\mathrm{CA}(z)$ *of a point* $z \in \mathbb{Z}^3$ *is the closed unit cube centered at this point with faces parallel to the coordinate planes, and the continuous analog of a set* $X \subseteq \mathbb{Z}^3$ *is defined as* $\mathrm{CA}(X) = \bigcup \{\mathrm{CA}(x) | x \in X\}$. *The (face) boundary of the continuous analog* $\mathrm{CA}(X)$ *of a set* $X \subseteq \mathbb{Z}^3$ *is noted* $\mathrm{bdCA}(X)$ *and is defined as the union of the set of closed faces each of which is the common face of a cube in* $\mathrm{CA}(X)$ *and a cube not in* $\mathrm{CA}(X)$.

Definition 5 (Well-composedness in 3D [4]) *A 3D set* $X \subseteq \mathbb{Z}^3$ *is well-composed iff* $\mathrm{bdCA}(X)$ *is a 2D manifold, i.e., a topological space which is locally Euclidian.*

Proposition 3 (No Critical Configurations [4]) *A set* $X \subseteq \mathbb{Z}^3$ *is well-composed iff the following critical configurations of cubes of type 1 or of type 2 (modulo reflections and rotations) do not occur in* $\mathrm{CA}(X)$ *or in* $CA(X^c)$ *(see Figure 1).*

We remark that if a set $X \subseteq \mathbb{Z}^3$ is well-composed, then X is locally 6-connected. The converse is false (see Figure 2).

Definition 6 (WC Gray-valued Maps) *We say that a 3D real-valued map* $u : \mathcal{D} \subseteq \mathbb{Z}^3 \mapsto \mathbb{R}$ *is well-composed if its strict cuts* $[u > \lambda]$ *and* $[u < \lambda]$, $\forall \lambda \in \mathbb{R}$, *are well-composed.*

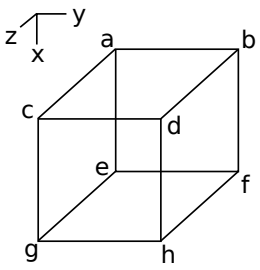

Fig. 3. The restriction $u\big|_S$ of u to a 3D block S.

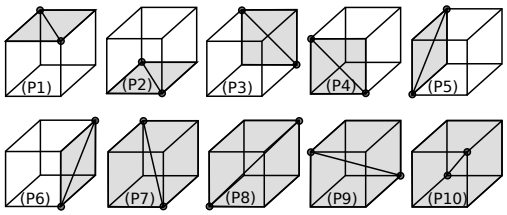

Fig. 4. The ten characteristical relations of well-composedness of a gray-valued image u restricted to a 3D block S.

To characterize 3D gray-level well-composed images, we first give two lemmas concerning the detection of the critical configurations of respectively type 1 and type 2.

Lemma 1 *The strict cuts* $[u > \lambda]$ *and* $[u < \lambda]$, $\lambda \in \mathbb{R}$, *of a gray-valued image* u *defined on a block* S, *such as depicted in Figure 3, do not contain any critical configurations of type 1 iff the six following properties hold:*

$\text{intvl}(a,d) \bigcap \text{intvl}(b,c) \neq \emptyset$ $(P1)$, $\quad \text{intvl}(e,h) \bigcap \text{intvl}(g,f) \neq \emptyset$ $(P2)$

$\text{intvl}(a,f) \bigcap \text{intvl}(b,e) \neq \emptyset$ $(P3)$, $\quad \text{intvl}(c,h) \bigcap \text{intvl}(g,d) \neq \emptyset$ $(P4)$

$\text{intvl}(a,g) \bigcap \text{intvl}(e,c) \neq \emptyset$ $(P5)$, $\quad \text{intvl}(b,h) \bigcap \text{intvl}(f,d) \neq \emptyset$ $(P6)$

Proof : Let us assume that one of these properties $(P_i), i \in [1,6]$, is false. Let us say it is the case of $(P1)$. Then two cases are possible: either $\max(a,d) < \min(b,c)$, and that means that there exists $\lambda = (\max(a,d) + \min(b,c))/2$ such that $[u < \lambda]$ contains the critical configuration $\{a,d\}$ (of type 1), or $\min(a,d) > \max(b,c)$, and there exists $\lambda = (\min(a,d) + \max(b,c))/2$ such that one more time $[u > \lambda]$ contains the critical configuration $\{a,d\}$. The reasoning is the same for all the other properties. Conversely, let us assume that there exists $\lambda \in \mathbb{R}$ such that either $[u > \lambda]$ or $[u < \lambda]$ contains a critical configuration of type 1. That means immediately that one of the 6 properties $P_i, i \in [1,6]$, corresponding to each of the six faces of the block S, is false (see Figure 4 for the faces and the corners concerned by the properties). □

Recall that the span of a set of values $E \subseteq \mathbb{R}$ is $\text{span}(E) = [\inf(E), \sup(E)]$.

Lemma 2 *The strict cuts* $[u > \lambda]$ *and* $[u < \lambda]$, $\lambda \in \mathbb{R}$, *of a gray-valued image* u *defined on a block* S *such as depicted in Figure 3, do not contain any critical configuration of type 2 iff the four following properties are true:*

$\text{intvl}(a,h) \bigcap \text{span}\{b,c,d,e,f,g\} \neq \emptyset$ $(P7)$

$\text{intvl}(b,g) \bigcap \text{span}\{a,c,d,e,f,h\} \neq \emptyset$ $(P8)$

$\text{intvl}(c,f) \bigcap \text{span}\{a,b,d,e,g,h\} \neq \emptyset$ $(P9)$

$\text{intvl}(d,e) \bigcap \text{span}\{a,b,c,f,g,h\} \neq \emptyset$ $(P10)$

Proof : Let us assume that one of these properties $(P_i), i \in [7,10]$, is false. Let us say it is the case of $(P7)$. Then two cases are possible:

- either $\max(a,h) < \min(b,c,d,e,f,g)$. Then there exists $\lambda = (\max(a,h) + \min(b,c,d,e,f,g))/2$ such that $[u < \lambda]$ contains the critical configuration $\{a,h\}$ (of type 2),
- or $\min(a,h) > \max(b,c,d,e,f,g)$. Then there exists $\lambda = (\max(b,c,d,e,f,g) + \min(a,h))/2$ such that (again) $[u > \lambda]$ contains the critical configuration $\{a,h\}$.
The reasoning is the same for all the other properties.
Conversely, let us assume that there exists $\lambda \in \mathbb{R}$ such that either $[u > \lambda]$ or $[u < \lambda]$ contains a critical configuration of type 2. That means immediately that one of the 4 properties $P_i, i \in [7,10]$, corresponding to each of the four diagonals of the block S, is false (see Figure 4). □

We are now ready to state the main theorem of this section, characterizing the well-composedness on a 3D gray-valued image.

Theorem 1 (Characterization of well-composedness in 3D) *Let us suppose that $\mathcal{D}$ is a hyperrectangle in $\mathbb{Z}^3$. A gray-valued 3D image $u : \mathcal{D} \mapsto \mathbb{R}$ is well-composed on $\mathcal{D}$ iff on any block $S \subseteq \mathcal{D}$, $u\big|_S$ satisfies the properties $(P_i), i \in [1,10]$.*

3 Local interpolations

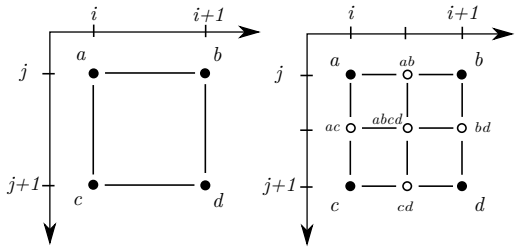

Fig. 5. Illustration of the subdivision process on a block S.

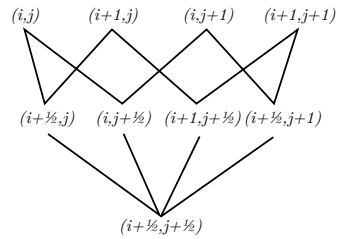

Fig. 6. $s(S) \subseteq \left(\frac{\mathbb{Z}}{2}\right)^n$ as a poset.

Using interpolations with one subdivision does not deteriorate the initial signal. The size of the original image is multiplied by a factor of 2^n, where n is the dimension of the space of the image. Figure 5 illustrates this subdivision process.

3.1 Subdivision of a Domain and $\left(\frac{\mathbb{Z}}{2}\right)^n$ as a poset

The subdivision of a block allows us to provide an order to the elements. Using this order, the subdivided space is a poset.

Let z be a point in $\mathbb{Z}^n$, and S_z its associated block. We define the subdivision of S_z as $s(S_z) = \{z' \in \left(\frac{\mathbb{Z}}{2}\right)^n \big| ||z - z'||_\infty \leq 1 \text{ and } \forall i \in [1,n], z'_i \geq z_i\}$. The

subdivision of a domain $\mathcal{D} \subseteq \mathbb{Z}^n$ is the union of the subdivisions of the blocks contained in $\mathcal{D}$, i.e., $s(\mathcal{D}) = \bigcup_{S \subseteq \mathcal{D}} s(S)$.

Definition 7 (Order of a point of $\left(\frac{\mathbb{Z}}{2}\right)^n$) *Assume e_i is a fixed basis of $\mathbb{Z}^n$. We note $\frac{1}{2}(z) = \{i \in [1,n] \big| z_i \in \frac{\mathbb{Z}}{2} \setminus \mathbb{Z}\}$. The sets $\mathbb{E}_k$, for $k \in [0,n]$, are defined such that $\mathbb{E}_k = \{z \in \left(\frac{\mathbb{Z}}{2}\right)^n \mid \left|\frac{1}{2}(z)\right| = k\}$ (where $\left|E\right|$ denotes the cardinal of the set E), and represent a partition of $\left(\frac{\mathbb{Z}}{2}\right)^n$. We call* order *of a point z the value k such that $z \in \mathbb{E}_k$ and we note it $\mathfrak{o}(z)$.*

Definition 8 (Parents in $\left(\frac{\mathbb{Z}}{2}\right)^n$) *Let z be a point of $\left(\frac{\mathbb{Z}}{2}\right)^n$. The set of the* parents *of $z \in \left(\frac{\mathbb{Z}}{2}\right)^n$, noted $\mathbb{P}(z)$, is defined by $\mathbb{P}(z) = \cup_{i \in \frac{1}{2}(z)} \{z - \frac{e_i}{2}, z + \frac{e_i}{2}\}$. The parents of $z \in \left(\frac{\mathbb{Z}}{2}\right)^n$ of order 0 are $\mathbb{P}^0(z) = \{z\}$ and of order $k > 0$ are defined recursively by $\mathbb{P}^k(z) = \cup_{p \in \mathbb{P}(z)} \mathbb{P}^{k-1}(p)$.*

Definition 9 ($\mathcal{G}(z)$ and $\mathbb{A}(z)$) *Let z be a point of $\left(\frac{\mathbb{Z}}{2}\right)^n$. The* ancestors *of $z \in \left(\frac{\mathbb{Z}}{2}\right)^n$ are $\mathbb{A}(z) = \mathbb{P}^{\mathfrak{o}(z)}(z)$. We set $\mathcal{G}(z) = \cup_{k \in [0, \mathfrak{o}(z)]} \mathbb{P}^k(z)$.*

Notice that $\mathbb{A}(z) \subseteq \mathbb{Z}^n$ and that any point $z \in \mathbb{E}_k$, $k \in [1,n]$, has its parents in $\mathbb{E}_{k-1}$. Hence $\{\mathbb{E}_k\}_{k \in [0,n]}$ is a (hierarchical) partition of $\left(\frac{\mathbb{Z}}{2}\right)^n$, and $(\left(\frac{\mathbb{Z}}{2}\right)^n, \mathbb{P})$ is a poset (see Figure 6).

Definition 10 (Opposites) *Let z be a point of $\left(\frac{\mathbb{Z}}{2}\right)^n$. The (set of)* opposites *of $z \in \left(\frac{\mathbb{Z}}{2}\right)^n$ is the family of pairs of points $\mathrm{opp}(z) = \cup_{i \in \frac{1}{2}(z)} \left\{\{z - \frac{e_i}{2}, z + \frac{e_i}{2}\}\right\}$.*

3.2 Interpolations with one subdivision

Let us recall that the convex hull $\mathrm{convhull}(Z)$ of a set of m points $Z = \{z^1, \ldots, z^m\} \subseteq \mathbb{Z}^n$ is:

$$\mathrm{convhull}(Z) = \left\{ \sum_{i=1}^{m} \alpha_i z^i \;\middle|\; \sum_{i=1}^{m} \alpha_i = 1 \text{ and } \forall i \in [1,m], \alpha_i \geq 0 \right\}$$

Definition 11 (Subdivision of edges, faces, and cubes) *Let $\mathcal{E} = \{z_1, z_2\}$ be an edge in $\mathbb{Z}^n$. The subdivision of $\mathcal{E}$ is $s(\mathcal{E}) = \{z \in \left(\frac{\mathbb{Z}}{2}\right)^n \big| z \in \mathrm{convhull}(\mathcal{E})\}$. The subdivision of a face $\mathcal{F} = \{z_1, z_2, z_3, z_4\}$ is $s(\mathcal{F}) = \{z \in \left(\frac{\mathbb{Z}}{2}\right)^n \big| z \in \mathrm{convhull}(\mathcal{F})\}$. The subdivision of a cube $\mathcal{C} = \{z_1, \ldots, z_8\}$ is $s(\mathcal{C}) = \{z \in \left(\frac{\mathbb{Z}}{2}\right)^n \big| z \in \mathrm{convhull}(\mathcal{C})\}$.*

3.3 A set of properties that an interpolation has to satisfy

An *interpolation* of a map $u : \mathcal{D} \subseteq \mathbb{Z}^n \mapsto \mathbb{R}$ to a map $\mathfrak{I}(u) : s(\mathcal{D}) \subseteq \left(\frac{\mathbb{Z}}{2}\right)^n \mapsto \mathbb{R}$ is a transformation such that $\mathfrak{I}(u)\big|_S = u\big|_S$ for any block $S \subseteq \mathcal{D}$.

Let $u : \mathcal{D} \subseteq \mathbb{Z}^3 \mapsto \mathbb{R}$ be any 3D gray-valued image. We say that an interpolation $\mathfrak{I} : u \mapsto \mathfrak{I}(u)$ is *self-dual* iff $\mathfrak{I}(-u) = -\mathfrak{I}(u)$. A self-dual interpolation

does not overemphasize bright components at the expense of the dark ones, or conversely.

An interpolation $\mathfrak{I} : u \mapsto \mathfrak{I}(u)$ in 3D is said *ordered* if the new values are inserted firstly at the centers of the subdivided edges, secondly at the centers of the subdivided faces, and finally at the centers of the subdivided cubes.

An ordered interpolation is said *in between* iff it puts the values at a point z in between the values of its parents $\mathbb{P}(z)$.

Finally, we say that an interpolation is *well-composed* iff the image $\mathfrak{I}(u)$ resulting from the interpolation of u is well-composed for any given image u.

We are interested in interpolations $\mathfrak{I}$ with the following properties.

$$(\mathcal{P}) \Leftrightarrow \begin{cases} \mathfrak{I} \text{ is invariant by translations, } \frac{\pi}{2}\text{'s rotations and axial symmetries} \\ \mathfrak{I} \text{ is ordered} \\ \mathfrak{I} \text{ is in-between} \\ \mathfrak{I} \text{ is self-dual} \\ \mathfrak{I} \text{ is well-composed} \end{cases}$$

3.4 The scheme of local interpolations verifying $\mathcal{P}$

A *local interpolation* $\mathfrak{I}$ is an interpolation such as for any block $S \subseteq \mathcal{D}$, $\mathfrak{I}(u)$ on $s(S)$ is computed only from its nearest neighbours belonging to $\mathbb{E}_0$ (we see an image as a graph). For convenience, we will write u' instead of $\mathfrak{I}(u)$ for local interpolations in the sequel.

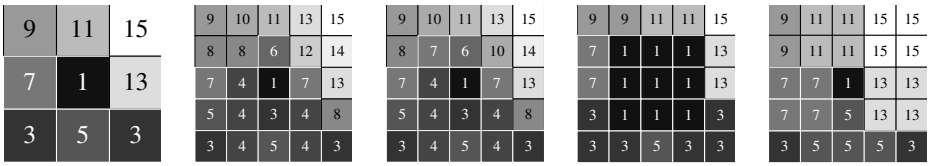

Fig. 7. From left to right: an image, and its interpolations with the *median*, the *mean/median*, the *min* and the *max*.

Lemma 3 (Local interpolation scheme) *Any local interpolation* $\mathfrak{I}$ *on* $\left(\frac{\mathbb{Z}}{2}\right)^n$ *verifying* $\mathcal{P}$ *can be characterized by a set of functions* $\{f_k\}_{k\in[1,n]}$ *such that:*

$$\forall\, z \in \left(\frac{\mathbb{Z}}{2}\right)^n,\ u'(z) = \begin{cases} u(z) & \text{if } z \in \mathbb{E}_0 \\ f_k(u|_{\mathbb{A}(z)}) & \text{if } z \in \mathbb{E}_k,\ k \in [1,n] \end{cases}$$

We denote such an interpolation $\mathfrak{I}_{f_1,\ldots,f_n}$.

Proof : The interpolation process on the subdivided edges depends only on the values of u at the vertices of the original edges due to the locality of the method. Furthermore it has to be invariant by axial symmetries and rotations.

Hence, there is a unique function f_1 characterizing the interpolation on the subdivided edges. The reasoning is the same on the faces and the cubes respectively for f_2 and f_3. □

Notice that it is an implication and not an equivalence: an interpolation verifying this scheme does not verify all the properties in $\mathcal{P}$.

3.5 I_0, I_{WC}, and I_{sol} for local interpolations

Let us introduce some useful sets to express recursively the local interpolations satisfying the properties $\mathcal{P}$.

Definition 12 (I_0 and definition of a local in-between interpolation) *Let $u : \mathcal{D} \mapsto \mathbb{R}$ be a gray-valued map, let z be a point of $s(\mathcal{D}) \setminus \mathbb{E}_0$, and let $\mathfrak{I}$ be a given local interpolation. We define the set $I_0(u, z)$ associated to $\mathfrak{I}$ by:*

$$I_0(u,z) \overset{(def)}{=} \bigcap_{\{z^-,z^+\}\in \mathrm{opp}(z)} \mathrm{intvl}(u'(z^-), u'(z^+))$$

Then, an ordered local interpolation $\mathfrak{I}$ is said in-between iff $u'(z) \in I_0(u, z)$ for any image $u : \mathcal{D} \mapsto \mathbb{R}$ and $z \in s(\mathcal{D}) \setminus \mathbb{E}_0$.

Definition 13 (I_{WC} and I_{sol}) *Let $u : \mathcal{D} \mapsto \mathbb{R}$ be a gray-valued image, z be a point of $s(\mathcal{D}) \setminus \mathbb{E}_0$, and $\mathfrak{I}$ be a given local interpolation. We define the set $I_{WC}(u, z)$ associated to $\mathfrak{I}$ such as for any $z \in \mathbb{E}_1$, $I_{WC}(u, z) = \mathbb{R}$ and for any $z \in \mathbb{E}_k$ with $k \geq 2$:*

$$I_{WC}(u,z) \;=\; \{\, v \in \mathbb{R} \;\mid\; u'(z) = v \;\Rightarrow\; u'\big|_{\mathcal{G}(z)} \text{ is well-composed} \,\}$$

Last, let us denote $I_{sol}(u, z) = I_0(u, z) \cap I_{WC}(u, z)$.

The following scheme is necessary to satisfy $\mathcal{P}$ (but not sufficient).

Theorem 2 *Any local interpolation $\mathfrak{I}$ satisfying $\mathcal{P}$ is such that:*

$$\forall z \in \left(\tfrac{\mathbb{Z}}{2}\right)^n, u'(z) = \begin{cases} u(z) & \text{if } z \in \mathbb{E}_0 \\ f_k(u\big|_{\mathrm{A}(z)}) \in I_{sol}(u,z) & \text{if } z \in \mathbb{E}_k, k \in [1,n] \end{cases}$$

Notice that such a local interpolation $\mathfrak{I}$ is ordered, in-between, well-composed, but not necessarily self-dual.

3.6 Determining f_1 for self-dual local interpolations

Let us begin with the study of f_1, *i.e.*, the function setting the values at the centers of the subdivided edges. This function has to be self-dual, symmetrical, and in-between. We choose one of the most common function satisfying these constraints: the mean operator $f_1 : \mathbb{R}^2 \mapsto \mathbb{R} : (v_1, v_2) \mapsto f_1(v_1, v_2) = (v_1 + v_2)/2$.

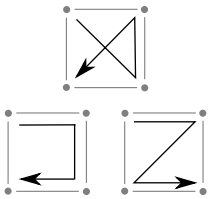

Fig. 8. The 3 possible configurations in 2D (modulo reflections and rotations).

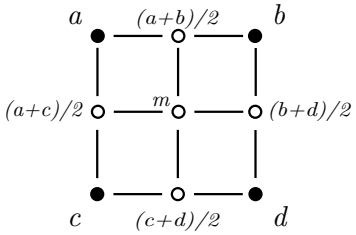

Fig. 9. $u'\big|_{\mathcal{G}(z)}$ for $z \in \mathbb{E}_2$ for any self-dual local interpolation after the application of f_1 (with m any value $\in \mathbb{R}$).

3.7 Equations of f_2 for self-dual local interpolations

Concerning f_2, *i.e.*, the function which sets the values of u' at the centers of the subdivided faces, let us compute $I_0(u, z)$ and $I_{WC}(u, z)$ for any given $z \in \mathbb{E}_2$ to deduce $I_{sol}(u, z)$. Their values depend on the *configurations* of $u\big|_{\mathbb{A}(z)}$.

Let us assume that $u\big|_{\mathbb{A}(z)} = \begin{pmatrix} a & b \\ c & d \end{pmatrix}$. Then a total of $4! = 24$ increasing orders are possible for these 4 values. Modulo reflections and axial symmetries, we obtain a total of 3 possible configurations: the α-*configurations* correspond to the relation $a \leq d < b \leq c$, the U-*configurations* to $a \leq b \leq d \leq c$, and the Z-*configurations* to $a \leq b \leq c \leq d$ (see Figure 8).

Lemma 4 *Let z be a point in $\mathbb{E}_2$. Modulo reflections and symmetries, an α-configuration implies that $u\big|_{\mathbb{A}(z)}$ is not well-composed, whereas a U- or Z-configuration implies that $u\big|_{\mathbb{A}(z)}$ is well-composed.*

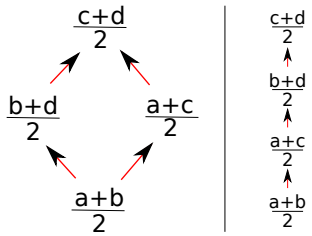

Fig. 10. The Hasse diagrams for the α- and the U-configurations (left) and for the Z-configuration (right).

Let us begin with the computation of $I_0(u, z)$ for $z \in \mathbb{E}_2$. From the values already set in u' on $\mathbb{P}(z) \subseteq \mathbb{E}_1$ by f_1 during the recursive process (see Fig-

ure 9), we can compute $I_0(u,z)$ using the Hasse diagram[3] for each configuration (see Figure 10). We obtain finally that $I_0(u,z) = \text{intvl}(\frac{a+c}{2}, \frac{b+d}{2})$ for the three configurations, with one important property: the median value of $u\big|_{\mathbb{A}(z)}$ always belongs to $I_0(u,z)$.

Let us follow with the computation of $I_{WC}(u,z)$, where $u'\big|_{\mathcal{G}(z)}$ (see Figure 9) satisfies four conditions:

$$\text{intvl}(a,m) \cap \text{intvl}((a+b)/2,(a+c)/2) \neq \emptyset, \quad (1)$$
$$\text{intvl}((a+b)/2,(b+d)/2) \cap \text{intvl}(m,b) \neq \emptyset, \quad (2)$$
$$\text{intvl}((a+c)/2,(c+d)/2) \cap \text{intvl}(m,c) \neq \emptyset, \quad (3)$$
$$\text{intvl}(m,d) \cap \text{intvl}((c+d)/2,(b+d)/2) \neq \emptyset. \quad (4)$$

In the case of the α-configuration, $(2) \Rightarrow m \leq \frac{b+d}{2}$ and $(4) \Rightarrow m \geq \frac{b+d}{2}$. That implies that $m = \frac{b+d}{2}$, which also satisfies (1) and (3). Consequently, $I_{WC}(u,z) = \{\text{med}\{u\big|_{\mathbb{A}(z)}\}\}$, and because $I_{WC}(u,z) \subseteq I_0(u,z)$, $I_{sol}(u,z) = \{\text{med}\{u\big|_{\mathbb{A}(z)}\}$ in the not well-composed case.

In the cases of the U- and the Z-configurations, we obtain that $I_{WC}(u,z) = [\frac{a+b}{2}, \frac{c+d}{2}] \supseteq I_0(u,z)$, so we conclude that $I_{sol}(u,z) = I_0(u,z)$.

Theorem 3 *Given an image $u : \mathcal{D} \mapsto \mathbb{R}$, any local interpolation $\mathfrak{I}_{f_1,f_2,f_3}$ satisfying $\mathcal{P}$ is such that $\forall\, z \in s(\mathcal{D}) \cap \mathbb{E}_2$:*

$$\begin{array}{ll} f_2(u\big|_{\mathbb{A}(z)}) = \text{med}\{u\big|_{\mathbb{A}(z)}\} & \text{if } u\big|_{\mathbb{A}(z)} \text{ is not W.C.,} \\ f_2(u\big|_{\mathbb{A}(z)}) \in I_0(u,z) & \text{otherwise.} \end{array}$$

Let z be a point in $s(\mathcal{D}) \cap \mathbb{E}_2$. Amongst the applications f_2 satisfying $\mathcal{P}$, there exists (at least) the *median method* (see Figure 7), consisting in setting the value of $u'(z)$ at $\text{med}\{u\big|_{\mathbb{A}(z)}\}$ (in this case f_2 is an operator and not only a function), the *mean/median method of Latecki* [6] consisting in setting the value $u'(z)$ at $\text{mean}\{u\big|_{\mathbb{A}(z)}\}$ in the well-composed case and to $\text{med}\{u\big|_{\mathbb{A}(z)}\}$ otherwise, and also the *min/max method*, consisting in setting the value $u'(z)$ at $\frac{1}{2}(\min\{u\big|_{\mathbb{A}(z)}\} + \max\{u\big|_{\mathbb{A}(z)}\})$ in the well-composed case and to $\text{med}\{u\big|_{\mathbb{A}(z)}\}$ otherwise.

3.8 Equations of f_3 for local self-dual interpolations

Theorem 4 *No local interpolation satisfies $\mathcal{P}$ for $n \geq 3$ with one subdivision as soon as we chose the mean operator to interpolate in 1D.*

Proof : Let z be the center of a subdivided cube. We have $u'\big|_{\mathbb{A}(z)}$ as in the Figure 11 (on the left). We apply the first interpolating function f_1, *i.e.*, we set

[3] Recall that a Hasse diagram is used to represent finite partially ordered sets with the biggest elements at the top

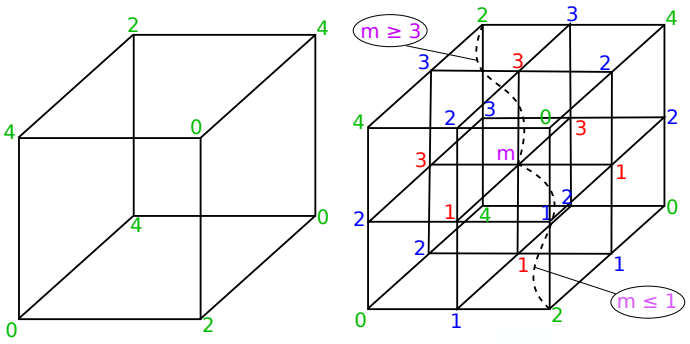

Fig. 11. A counter-example proving that a local interpolation satisfying $\mathcal{P}$ with one subdivision can not ensure well-composedness (the values of u' on $\mathbb{E}_0$ are in green, the ones on $\mathbb{E}_1$ are in blue, the ones on $\mathbb{E}_2$ are in red, and the ones on $\mathbb{E}_3$ are in purple).

the values of u' at the centers of the subdivided edges at the mean of the values on the vertices. Then we apply the second interpolating function f_2, which fixes the values of u' at the centers of the subdivided faces at the median of the values of u' at the four corresponding corners (because u is well-composed on none of the faces of the cube). Finally, referring to the properties that a function u' has to satisfy to be well-composed (see theorem 1), f_3 must also satisfy the constraints $c \geq 3$ and $c \leq 1$ (both are constraints of type 2) that are incompatible. So, no local interpolation of this sort can satisfy the set of constraints $\mathcal{P}$ as soon as $n \geq 3$. □

4 Conclusion

In this paper, we have presented a characterization of well-composedness for 3D gray-valued images. We proved that no local interpolation satisfying $\mathcal{P}$ with one subdivision is able to make 3D well-composed images as soon as we choose the mean operator as interpolation in 1D.

Although our formalism is developped in the continuous domain (the interpolations take their values in $\mathbb{R}$), it is in fact a discrete setting. Indeed, the image u' can easily be computed in $\mathbb{Z}$ as soon as the space image of u is also $\mathbb{Z}$. We just have to multiply the values of the original image u by a factor $k \in \mathbb{Z}$ where k depends on the interpolation we use (e.g., $k = 2$ for the median method and $k = 4$ for the mean/median method in 2D). Another way to deal with images having values in $\mathbb{Z}/k$ is to use a generic image processing library [7].

Future research should tackle the two following directions. The first direction is to use an alternative to f_1 such as $(a, b) \mapsto \text{med}(a, b, c)$ (where c is the center of the space of the image u). The second direction is to use a non-local approach, *e.g.*, a front propagation algorithm. In that case, we do not have to use any systematic operator f_1 anymore, nor to use an ordered interpolation. First results in this second direction are promising.

References

1. Caselles, V., Monasse, P.: Geometric Description of Images as Topographic Maps, Lecture Notes in Mathematics, vol. 1984. Springer-Verlag (2009)
2. Géraud, T.: Self-duality and discrete topology: Links between the morphological tree of shapes and well-composed gray-level images. Journée du Groupe de Travail de Géométrie Discrète (June 2013), http://jgeodis2013.sciencesconf.org/conference/jgeodis2013/program/JGTGeoDis2013Geraud.pdf
3. Géraud, T., Carlinet, E., Crozet, S., Najman, L.: A quasi-linear algorithm to compute the tree of shapes of n-D images. In: Hendriks, C.L., Borgefors, G., Strand, R. (eds.) Mathematical Morphology and Its Application to Signal and Image Processing – Proceedings of the 11th International Symposium on Mathematical Morphology (ISMM). Lecture Notes in Computer Science Series, vol. 7883, pp. 98–110. Springer, Heidelberg (2013)
4. Latecki, L.: 3D well-composed pictures. Graphical Models and Image Processing 59(3), 164–172 (May 1997)
5. Latecki, L., Eckhardt, U., Rosenfeld, A.: Well-composed sets. Computer Vision and Image Understanding 61(1), 70–83 (January 1995)
6. Latecki, L.J.: Well-composed sets. In: Advances in Imaging and Electron Physics. vol. 112, pp. 95–163. Academic Press (2000)
7. Levillain, R., Géraud, T., Najman, L.: Writing reusable digital topology algorithms in a generic image processing framework. In: Köthe, U., Montanvert, A., Soille, P. (eds.) WADGMM 2010. Lecture Notes in Computer Science Series, vol. 7346, pp. 140–153. Springer-Verlag Berlin Heidelberg (2012)
8. Marchadier, J., Arquès, D., Michelin, S.: Thinning grayscale well-composed images. Pattern Recognition Letters 25, 581–590 (April 2004)
9. Najman, L., Géraud, T.: Discrete set-valued continuity and interpolation. In: Hendriks, C.L., Borgefors, G., Strand, R. (eds.) Mathematical Morphology and Its Application to Signal and Image Processing – Proceedings of the 11th International Symposium on Mathematical Morphology (ISMM). Lecture Notes in Computer Science Series, vol. 7883, pp. 37–48. Springer, Heidelberg (2013)
10. Ngo, P., Passat, N., Kenmochi, Y., Talbot, H.: Topology-preserving rigid transformation of 2d digital images. IEEE Transactions on Image Processing 23(2), 885–897 (February 2014)
11. Rosenfeld, A.: Connectivity in digital pictures. Journal of the ACM 17(1), 146–160 (January 1970)